MPC Published by ASTM

Dear Author,

YOUR PAGE PROOF IS AVAILABLE IN PDF FORMAT; please refer to this URL address
http://115.111.50.156/jw/AuthorProofLogin.aspx?pwd=5ddad2de8d9b&CA=AT

███████████████████████

████████████████████

The site contains 1 file. You will need to have Adobe Acrobat Reader software to read these files. This is free software and is available for user downloading at http://www.adobe.com/products/acrobat/readstep.html.

This file contains:
Adobe Acrobat Users - NOTES tool sheet
A copy of your page proofs for your article

Please read the page proofs carefully and:

1) indicate changes or corrections using e-annotation;
2) answer all queries;
3) proofread any tables and equations carefully;
4) check that any special characters have translated correctly.

Special Notes:

Your edits must be returned (uploaded or emailed) within 48 hours of receiving page proofs to review. Please notify Denise Stanley (denise.stanley@cenveo.com) immediately if you anticipate a delay in returning your edits.

Your Login and Password are valid for a limited time. Your prompt attention to and return of page proofs will help expedite publication of your work. Thank you for your cooperation.

If you have any questions regarding your article, please contact me. PLEASE ALWAYS INCLUDE YOUR ARTICLE NO. (MPC20120016.R1) WITH ALL CORRESPONDENCE.

Posting Author Papers on Website Policy—Author's Rights as Stipulated in the Accepted Electronic Agreement during Paper Submission:

"The right to post the pre-print version of the Work on your website or your employer's website with reference to the publication by ASTM as the copyright holder. This preprint will be sent to you by the copyeditor. This version

does not include the final edits. Such preprints may be posted as electronic files on the Author's own website for personal or professional use, or on the Author's internal university or corporate networks/intranet, or secure external website at the Author's institution, but not for commercial sale or for any systematic external distribution by a third party (eg: a listserver or database connected to a public access server). Prior to publication, the Author must include the following notice on the preprint: "This is a preprint of an article accepted for publication in (Journal Title Copyright @ (year) (copyright ASTM International, West Conshohocken, PA)". After publication of the Work by ASTM International, the preprint notice should be amended to read as follows: "This is a preprint of an article published in (include the complete citation information for the final version of the Work as published in the print edition of the Journal)" and should provide an electronic link to the Journal's WWW site, located at the following ASTM URL: http://www.astm.org. The author agrees not to update the preprint or replace it with the published version of the Work."

Sincerely,
Denise Stanley, Journal Production Manager
E-mail: Denise.Stanley@cenveo.com

AUTHOR QUERY FORM

Dear Author,

Below are the queries associated with your article; please answer all of these queries before sending the proof back to Cenveo. Author please indicate the correct color processing option from the list below:

1. Author, please confirm Figure number(s) that should appear as color in print. Please know that any associated mandatory fees will apply for figures printed in color.

2. Author, please confirm Figure number(s) that should appear as color online only, there will be no fees applied.

3. Author, your paper currently does not include any color figures for online or print. If color is needed please indicate which figures it should be applied to and whether it is color in print or online.

Location in article	Query / Remark: click on the Q link to navigate to the appropriate spot in the proof. There, insert your comments as a PDF annotation.
AQ1	Please advise whether reference 32 was meant here instead of 22.
AQ2	Please advise – reference 54 citation deleted here as there is no reference 54 in the list.
AQ3	For reference 1, please provide dates and location of meeting.
AQ4	For reference 20, please check standard number, year, and name of organization.
AQ5	Please provide all authors for references 38 and 49.
AQ6	For the website references, please check that the date the sites were last accessed are correct. If not, please provide correct dates. Please provide the date for all website references.

Thank you for your assistance.

Adil Saeed,[1] *Zulfiqar A. Khan,*[2] *and Eliza L. Montgomery*[3]

Corrosion Damage Analysis and Material Characterization of Sherman and Centaur— The Historic Military Tanks

ABSTRACT: A study of corrosion damage and material characterization of two historic military tanks, the Sherman and Centaur is reported. Experiments were conducted to analyse surface corrosion and corrosion propagation from surface to sub-surface. Significant surface corrosion was found, and this phenomenon was further facilitated by delamination failure mechanisms. Corrosion depth for the Sherman was approximately $110\,\mu m$, where sulphide inclusions were detected in the sub-surface analysis. The Centaur's analysis showed corrosion pits at $100\,\mu m$ depth. These pits possess random geometrical configurations with evidence of sulphur, sodium, and calcium.

Introduction

The Tank Museum in Bovington, United Kingdom has one of the largest collections of military tanks from the First and Second World Wars and from post-war conflicts. These historic vehicles are at risk of aging because of corrosion. Historic military vehicles and other large mechanical museum artefacts are key entities, which provide a wealth of information and insight into past design processes, design methods, materials, and manufacturing techniques. Historic vehicles in the Tank Museum at Bovington are kept in two distinct environments, indoors (controlled) and outdoors (uncontrolled). Some of the vehicles run occasionally after being kept in the controlled environment in the museum. This temporary change in environment of the vehicles combined with other operating factors poses significant risk of failures.

The indoors environment refers to the controlled environment inside the Tank Museum. The lighting source is natural daylight combined with fluorescent lighting, which emits a low amount of ultraviolet (UV) light. The temperature is controlled in winter only and humidity is not controlled during any season. The outdoor environment refers to the uncontrolled environment that exists naturally in Bovington, United Kingdom. Bovington is in the county of Dorset on the south-western coast of England and is located approximately 9 km north of the English Channel.

[1]Sustainable Design Research Centre, School of Design, Engineering and Computing, Bournemouth Univ. Talbot Campus, Poole, Dorset BH12 5BB, United Kingdom (Corresponding author), e-mail: asaeed@bournemouth.ac.uk

[2]Ph.D., Sustainable Design Research Centre, School of Design, Engineering and Computing, Bournemouth Univ. Talbot Campus, Poole, Dorset BH12 5BB, United Kingdom, e-mail: zkhan@bournemouth.ac.uk

[3]Ph.D., Materials Testing and Corrosion Control Branch, National Aeronautics and Space Administration, Kennedy Space Center, FL 32899, United States of America, e-mail: eliza.l.montgomery@nasa.gov

2   MATERIALS PERFORMANCE AND CHARACTERIZATION

Structural deterioration through corrosion damage in large metal structures such as ships, air-craft, and bridges, is a colossal predicament [1,2], and large metal museum artefacts are no exception to this. The dilemma of corrosion damage in historic military tanks in the Tank Museum can be classified as one of the major perils to their structural integrity.

This paper presents results of corrosion on the surface, its propagation from surface to sub-surface, and the subsequent damage to the structural integrity of the Sherman M4A1 and/or the Centaur A27L. Both the Sherman and Centaur participated in the Second World War and post-war conflicts, encountered opponents' explosive attacks, and operated in a wide variety of terrains ranging from desert to Eastern Europe and therefore accumulated various types of structural damage during their service lives. Now kept in a museum, these vehicles still go through structural degradation because of corrosion. Sustainable methods are required to diminish corrosion and corrosion-related problems in these historic vehicles to preserve them for the current and coming generations keeping their cultural biography intact.

This is the first research conducted to evaluate corrosion on historic military tanks kept in the Tank Museum at Bovington. There is insufficient data on the tanks concerning their past exposure during the wars, their locations, and their operating environments, and it is beyond the scope of this research work to track their service history. However, war-related damage is significant on many of the tanks and the majority of the tanks display failures in the protective coatings.

It is important to slow down the process of structural degradation caused by corrosion failures or stop it wherever possible. It is, however, of critical importance that such measures are sustainable in terms of not compromising the historic and cultural heritage of these vehicles by excessive repair, replacements, and other maintenance techniques such as coatings. The sustainable conservation of these artefacts would include full understanding of the critical parameters that are responsible for initiating and accelerated propagation of corrosion. Linking these critical attributes to controlled environment facilities to optimise their design for achieving these goals economically is the objective of the present research.

It is, however, not possible to achieve controlled environments for all 300 plus vehicles; therefore, alternative methodologies can be devised for vehicles kept in uncontrolled facilities to slow down the process of structural degradation to minimise historic loss.

Findings from the undertaken research will enable the design of a sustainable framework of conservation of these vehicles in both controlled and uncontrolled environments.

Experimental Methodology
Sample Selection
Sherman M4A1

Sherman M4A1 was designed by Lima Locomotives in 1941–1942 in the United States and was utilised by the British Army in the Second World War [3,4]. This Sherman was provided by Royal Armoured Corps Gunnery School, Lulworth Camp, United Kingdom in 1955 to the museum. No images were taken with a view to identify specific areas of corrosion at that time or afterwards. This tank operated occasionally and is now inside the museum in a controlled environment. Inside the museum, the temperature is kept under control in winter only, and no control of relative humidity is exercised in any weather. The Sherman experiences medium levels of corrosion.

Sample was collected from the hull (turret area) of the Sherman. The exposed surface of the sample had a coating. However, the inner side was corroding and any previously applied coating had completely failed.

Centaur A27L

This tank was designed by the Leyland Motors in the United Kingdom in 1942–1945 and served in the Second World War [3,4]. This tank was given to the museum by the Ministry of Defence (MOD) in 1994. Again, there was no corrosion study conducted at the time of accession. Since 1994, this vehicle is stationary outside the museum in an uncontrolled environment. The Centaur is stationed outside the museum and is exposed to environmental conditions such as direct UV light from the sun, fluctuations in temperature and humidity, and varying times of wetness. The Centaur is undergoing extensive structural degradation. Figure 1 show the Centaur's armoured skirt, extensively affected by corrosion.

A sample was collected from the armoured skirt of the Centaur. The sample was coated on the exposed surface, whereas the inner side (towards the tracks) was corroding with little evidence of previously applied coating.

Samples' Materials Characterisation

Both samples were sectioned and x-ray fluorescence (XRF) was conducted at the cross section (newly exposed surface) of the samples to obtain the materials composition. XRF results illustrated that Sherman composition was approximately matching AISI 1000, and the Centaur was matching AISI 4000 series steel [5,6]. These materials were processed before/during the Second World War.
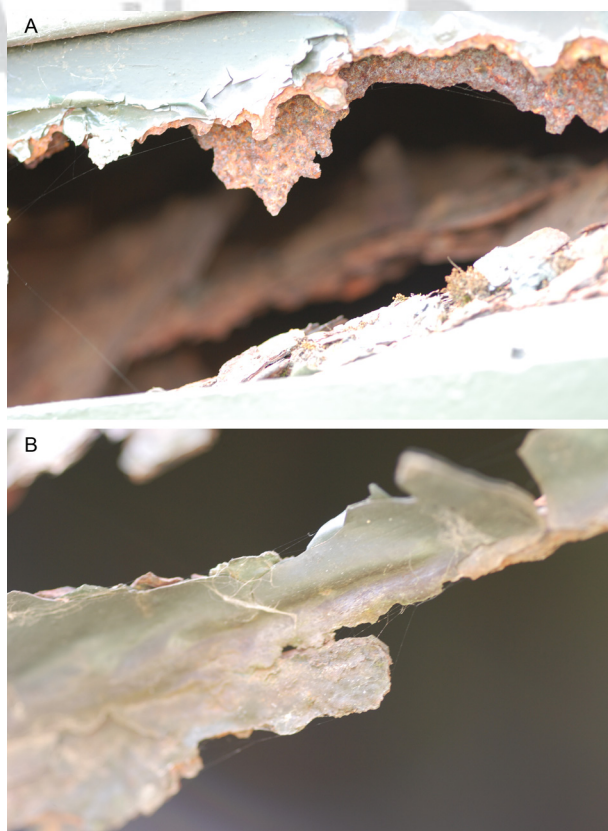

FIG. 1—*Corrosion in Centaur's armoured skirt to a significant level.*

4   MATERIALS PERFORMANCE AND CHARACTERIZATION

Sample Preparation

For sub-surface analysis, samples were sectioned, and then mounted in bakelite. Polishing was performed using silicon carbide abrasive papers. Samples were conditioned with a diamond suspension spray of 3 μm, rinsed with water, and then dried. No chemical treatment on samples was performed.

Sample Analysis

Scanning electron microscopy (SEM) and energy dispersive x-ray spectroscopy (EDS) were performed under high vacuum using field emission gun scanning electron microscopy (FEGSEM) at 20 kV. Samples were conductive and therefore required no carbon coating for the analysis. EDS calibration was conducted with Cu standard, a normal practice for EDS calibration. SEM examination obtained micro-structural characteristics of the samples in high resolution. Through EDS, a qualitative and quantitative determination of the elements was obtained and evaluated from the energy spectrum versus relative counts of the detected x rays [7,8].

First, SEM and EDS analyses were performed on the corroded surfaces of each tank, which had no effective protection (paints/coatings). Second, analysis was performed at the cross section of the samples, where corrosion propagation from surface to sub-surface, corrosion pitting (a form of localised corrosion confined to a small area, which results in cavities), and cracking were all prevalent.

Results and Discussion
Sherman M4A1

On the corroding surface of the Sherman in total six elements, Iron (Fe), Calcium (Ca), Silicon (Si), Aluminium (Al), Sodium (Na), and Oxygen (O), were identified at three spectra. EDS results of these three spectra are provide in Table 1. In spectrum 1, high proportion of O (46.01 wt. %) was recorded. Fe (44.22 wt. %) was recorded lowest at spectrum 2.

X-ray fluorescence (XRF) results at the cross section of the sample illustrated Fe (98.30 wt. %), Mn (0.63 wt. %), and Si (0.65 wt %) as the main elements [5]. Si originates from alloying elements. The detection of Al on the corroding surface could be attributed to the Al-based paint protection applied at some stage. Ca and Na in spectra 1 and 2 are surface contaminants and originate from previous/current atmospheres.

Further investigations were conducted to obtain corrosion propagation from surface to sub-surface, shown in Fig. 2. Significant corrosion was recorded that has resulted in delamination of corrosion residues from the surfaces. The surface was affected to a depth of almost 110 μm into the bulk metal, where sub-surface cracks were also identified. Corrosion was investigated at the cross section of the corroding edge, labelled as spectrum 1, shown in Fig. 2(*a*), and at the bulk metal

TABLE 1—*Sherman EDS point analysis of corroding surface.*

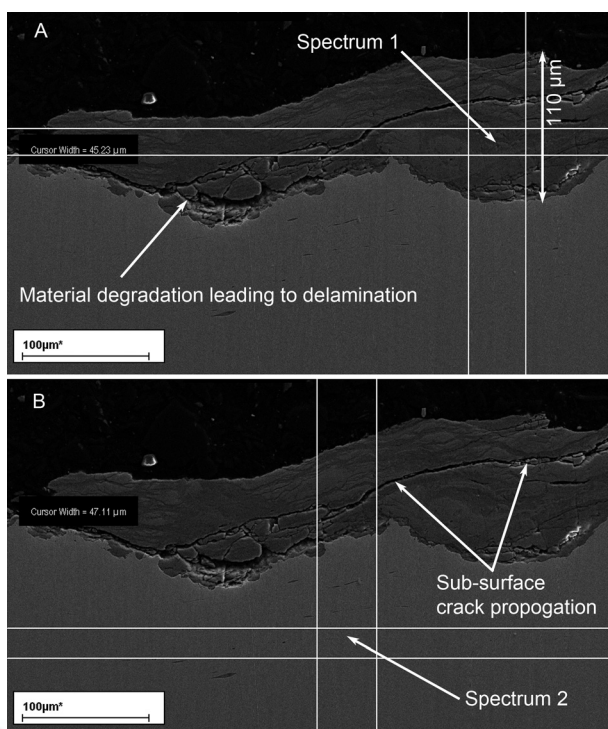| Sample: Sherman-corroding Surface (Results in Weight %)					
Processing Option: All Elements Analysed/Normalised					
Spectrum No.	O	Na	Al	Si	Ca	Fe
---	---	---	---	---	---	---
1	46.01	0.00	3.02	4.62	1.19	45.13
2	41.55	1.05	6.55	5.67	0.93	44.22
3	39.98	0.00	1.46	1.16	0.00	57.38

FIG. 2—*Sherman cross section—rectangular area shows EDS analysis area (approximately 820 μm²): (a) CP to 110 μm, and materials' delamination, and (b) sub-surface crack propagation.*

where no corrosion was occurring, labelled as spectrum 2, shown in Fig. 2(*b*). In spectrum 1, Fe (60.84 wt. %), Mn (0.45 wt. %), Ca (0.40 wt. %), and O (38.30 wt. %) were detected. The presence of a high amount of oxygen and traces of Ca show that drastic corrosion has occurred. Oxygen is the signature for iron oxide (FeO) corrosion product formation, and Ca is known to be present in atmospheric salt deposits as well as sea salt [9,10]. At spectrum 2, where no corrosion has propagated yet, only Fe (99.41 wt. %) and Mn (0.58 wt. %) were detected.

Figure 2 demonstrates corrosion on the Sherman resulting in cracks and delamination of the material. Such surfaces, when exposed to stresses, will become one possible cause of structural failure [11], these are referred to as both mechanical (stresses because of dynamic and/or static loading) and corrosion-induced (stress corrosion cracking) stresses.

Sulphide inclusions were identified in the cross section from the Sherman, shown in Fig. 3. Spectrum 1 results showed Fe only 5.31 wt. % with a high amount of sulphur (S) (35.25 wt. %), other elements found at spectrum 1 were Mn (57.71 wt. %) and Fluorine (F) (1.70 wt. %). Spectrum 2, which was conducted at the metal, demonstrated Fe (99.24 wt. %) and Mn (0.75 wt. %). Spectrum 3 was conducted at the second inclusion and showed Fe (24.14 wt. %) with S (26.37 wt. %), Mn (46.95 wt. %), and F (2.52 wt. %). F can be classified as a surface contaminant that has possibly come into contact with the tank's surfaces during the war. F belongs to a halogen group of elements and is highly poisonous yellow gaseous element. Elemental F and F ion are highly toxic and can even react with inert noble gases such as krypton and xenon [12].

Sulphur in the Sherman originates from the steel-making process and Mn is an alloying agent [13], being added to steel to avoid FeS formation and to form MnS for the purpose of
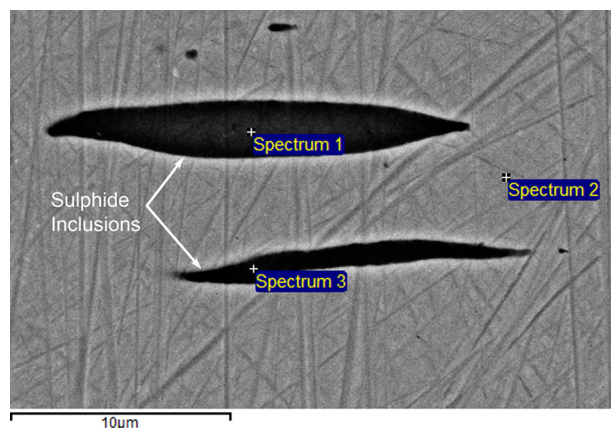
FIG. 3—*Sherman cross section—sulphide inclusions and EDS (point analysis) at 3 spectra.*

segregating S. MnS has a higher melting point and is chemically stable, and also during hot rolling 142
prevents the formation of FeS along the grain boundaries [14,15]. MnS inclusions tend to provide 143
better machining, increased wear resistance of the components, and reduced costs during product 144
manufacturing [16]. However, MnS inclusions cause the initiation of corrosive pits in bulk metal, 145
such as carbon steel and low carbon steel [17]. In addition, combined with corrosive environments, 146
these inclusions result in accelerated pit formation and deterioration of the overall corrosion resist- 147
ance of the metals [17–19]. 148

The temperature in the museum is kept between 18–25°C in winter. The buildings where the 149
tanks are housed are not humidity controlled apart from being enclosed and protected from direct 150
atmospheric moisture. Recording of temperatures and relative humidity (RH) started in October 151
2011 in five locations and another five locations were included in early 2012 in the museum. The 152
recent monitoring, over a period of 4 months, indicate temperature fluctuations from 17°C to 20°C 153
and daily range of RH was reported to be from a low of 40 % to a high of 80 %. All of the 10 154
locations detected conditions where RH reached above 70 % at various intervals of time during a 155
24 h period. 156

There is plenty of evidence of condensation inside some areas in the museum where water regu- 157
larly runs off the tank's surfaces. Figure 4 illustrates the temperature and RH recorded in the WW2 158
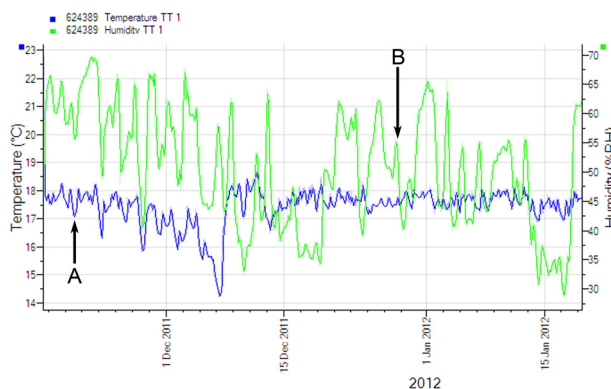

FIG. 4—*Temperature (a), and RH (b) graphs in WW2 Hall where Sherman is kept.*

hall where the Sherman is kept. In first reading during 25/2010/2011–16/2011/2011, highest and lowest temperatures recorded were ∼23°C and ∼16.5°C with highest RH being ∼80 % and the lowest being ∼53 %. In the second reading (Dec. 1, 2011– Jan. 15, 2012), the highest and lowest temperatures were ∼18.50°C and ∼14°C, respectively, as shown in Fig. 4. RH recorded during the same duration was just above 65 % RH as the highest and ∼30 % RH the lowest.

Corrosion is hugely influenced by the environment; in turn, this is attributed to the atmospheric pollutants [13]. Condensation is known to occur when temperatures exceed 0°C with 80 % RH [20], thus leading to a longer time of wetness (TOW) and atmospheric corrosion [21,22]. Therefore, during these temperature and RH combinations some degree of corrosion is expected in tanks in the museum. In addition, the critical RH will also decrease significantly in the presence of airborne as well as surface pollutants [23].

Under wet/damp conditions ($T \geq 0$ and RH > 80 %) and when the air is saturated with water vapour, dissolution of MnS inclusions are possible leading to the formation of corrosion pits. Sulphide inclusions identified in the bulk metal of the Sherman are likely points of weakness along the grain boundaries and will promote pitting corrosion; dissolution is expected at the edge of the inclusions through the formation of rust of sulphur over the inclusions and at the surrounding bulk steel. Changes in the shapes of the inclusions and the formation of microscopic cracks are also likely. The metal matrix is exposed when MnS dissolution occurs; the consequent dissolution products, i.e., elemental sulphur, thio-sulphate ion ($S_2O_3{}^{2-}$), hydrogen sulphide (H_2S), and hydrogen sulphide ion (HS^-) create a corrosive environment, encouraging pit propagation, and faster corrosion will also result [14,19,22,24–26]. Steel, stainless steel, and copper are all known to suffer from stress corrosion cracking and sulphide stress cracking because of free sulphides [27].

The identification of Na, Ca, and F on the surfaces is not favourable, whether accumulated from the air or the places where the tanks operated in the past. These will form corrosive electrolytes on the bare surfaces of the Sherman, consequently accelerating corrosion. Rusting will form on the surfaces from the precipitation of ferric oxide (Fe_2O_3). This rust is composed of the first oxy-hydroxide lepidocrocite (γ-FeOOH) and goethite (α-FeOOH), which consists of pores, cracks, and have poor adherence. Such rust layers formed on steel do not have the ability to form a protection against the corrosive products reaching the steel substrate and therefore will not effectively restrict the diffusion process [13,28–31].

Under current environmental conditions, when the RH reaches above 80 % and in the presence of surface contaminants, it is likely that corrosion in the Sherman will prevail resulting in structural failures.

Centaur A27L

Ultrasonic scanning to record the material loss because of corrosion has already been reported for the Centaur [5]. Table 2 illustrates results from ultrasonic scanning for the maximum and minimum remaining thicknesses at five points each. The difference between maximum and minimum points provides relative measure of corrosion as less thickness indicates more corrosion and vice

TABLE 2—*Centaur ultrasonic scanning results of the five lowest and highest remaining thicknesses.*

Centaur Sample's Dimension Length: 240 mm, Width: 96 mm									
Remaining thickness in mm	2.30	3.60	3.80	3.90	4.0	6.80	6.90	7.0	9.20	9.80
No. of occurrences of the remaining thicknesses	1	2	5	3	2	374	410	201	2	1

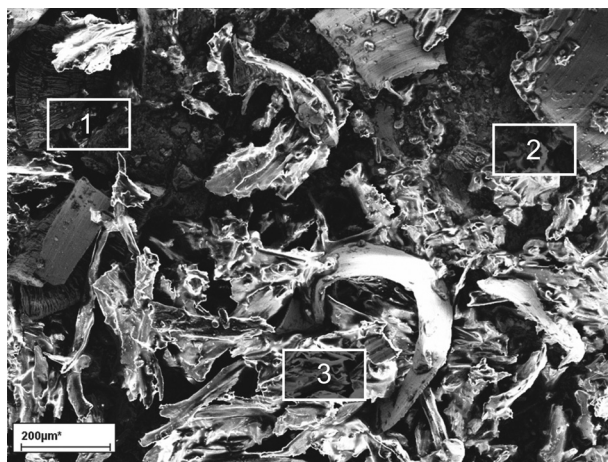8   MATERIALS PERFORMANCE AND CHARACTERIZATION

FIG. 5—*Centaur armoured skirt sample—corroding surface and EDS spectra locations.*

versa. At the time of manufacture, the maximum and minimum armour thicknesses for the Cen- 197
taur were 76 mm and 20 mm, respectively [3,4]. In the collected sample from the armoured skirt 198
the highest thickness was recorded as 9.80 mm. No higher value was detected after repeated scan- 199
ning. Values in Table 2 provide an understating of the armoured decay as the thickness has been 200
reduced significantly. Material loss of 7.50 mm has been recorded between the maximum and mini- 201
mum remaining thicknesses of 9.80 mm and 2.30 mm, respectively. 202

  The corroding surface was measured at three different spectra 1, 2, and 3 as shown in Fig. 5. 203
The experimental results of the state of corrosion measured at these spectra are presented in 204
Table 3. The surface was actively corroding and the protective coatings were severely degraded. 205
Experimental results from the above three spectra have shown that four elements Fe, Si, Al, and O 206
were present. Spectrum 1 indicated a high amount of corrosion product because of a high concen- 207
tration of O, which was responsible for the oxidation of Fe. Fe was recorded 56.25 wt. % at this 208
spectrum. The experimental results have found other elements such as Al and Si within the same 209
corrosion spectrum. Results from spectrum 2 has shown highest corrosion damage comparing to 210
spectra 1 and 3. The highest Fe concentration has been recorded in spectrum 3 with Si, Al, and O. 211

  Previous studies [6] have shown elements such as Fe, Cr, Mn, Ni, and Si through XRF analysis 212
of the cross section of the Centaur sample. Again Si originates from alloying elements and Al as a 213
residue from passivation treatment (Al-based coating) applied during/after the Centaur service life. 214

  Corrosive pits of random sizes were identified approximately 100 μm deep in the cross section 215
of the sample illustrated in Fig. 6. Nickel (Ni), Fe, Mn, Chromium (Cr), Ca, S, Si, Al, and O were 216

TABLE 3—*Centaur EDS points analysis results of corroding surface.*

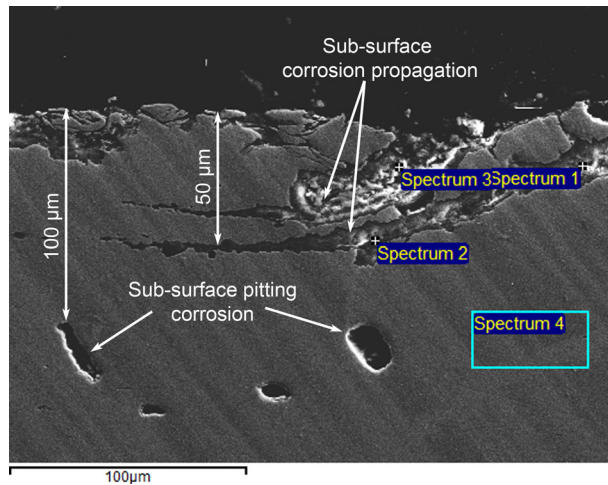| Sample: Centaur-corroding Surface (Results in Weight %)				
Processing Option: All Elements Analysed/Normalised				
Spectrum No.	O	Al	Si	Fe
1	36.58	3.97	3.18	56.25
2	36.88	22.34	5.04	35.72
3	28.06	2.15	4.09	65.67

FIG. 6—*Centaur cross section—location of EDS points, corrosion propagation, corrosion pits, and cracks.*

identified at four spectra and their results are given in Table 4. Spectra 1, 2, and 3 are of the corro- [217]
sion product layer, which clearly shows the high amount of oxygen versus elemental iron. Fe was [218]
recorded only 18.75 wt. % in the crack in spectrum 2 as shown in Fig. 6. O, Ca, and S are present in [219]
considerable amounts and will form localised zones of corrosion to propagate any cracks preferen- [220]
tially across the bulk metal grain boundaries leading to delamination of the surface material. Spec- [221]
trum 4 was selected at the bulk metal and has been located approximately 50 μm below the [222]
interface of the corrosion product layer and the bulk metal. Results from this spectrum have shown [223]
alloying elements only. Corrosion propagation of approximately 50 μm deep from surface to sub- [224]
surface was observed in this sample. [225]

 A sub-surface crack was identified in the cross section of the Centaur, shown in Fig. 7. Results [226]
from the EDS investigations are provided in Table 5. Spectra were measured at the crack and at the [227]
bulk area surrounding this crack. At spectra 1 and 2, only the alloying elements were identified and [228]
no O or Al was detected. However, in the crack, O was present. It is likely that this crack will prop- [229]
agate when subjected to stresses and/or fatigue. [230]

 Figures 6 and 8 illustrate a localised form of corrosion pits associated with surface corrosion. [231]
AQ1 Pits are widespread and their formation into cracks/cavities can be observed in Fig. 8 [32]. The for- [232]
mation of pits in two phases, (a) meta-stable and (b) stable pits, has been extensively reported [233]

TABLE 4—*Centaur EDS (point analysis) results of cross section.*

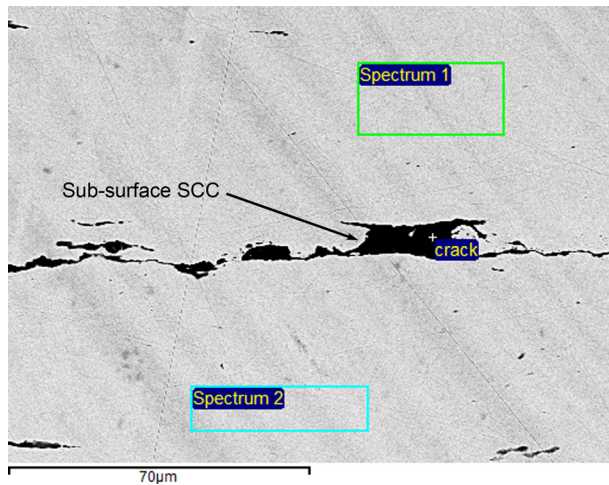| Sample: Centaur—Cross Sectional Surface (Results in Weight %)								
Processing Option: All Elements Analysed/Normalised								
Spectrum No.	O	Al	Si	S	Ca	Cr	Mn	Fe	Ni
1	40.39	0.29	3.39	0.40	1.71	1.30	2.00	49.88	0.60
2	39.86	1.05	14.12	0.29	0.47	1.35	24.06	18.75	0.00
3	41.14	0.00	0.57	0.76	1.85	5.52	0.68	47.94	1.50
4	0.00	0.00	0.41	0.00	0.00	1.87	0.46	96.50	0.74

FIG. 7—*Centaur cross section sub-surface crack and EDS points.*

[14,25,33–36]. Initially because of non-linear coupling between the dissolution of the metal and the [234] electrolyte composition, the formation of the pit takes place: (a) after which pit may propagate for [235] a short period and then die-down (meta-stable pit), or (b) it may continue propagating indefinitely, [236] known as stable pit, depending on the local fluctuations in the hydrodynamic boundary layer [237] [14,33,34]. [238]

The Centaur is exposed to rain, sea winds, and temperature fluctuations. Consequently, with [239] time, the sizes of the pits in Figs. 6 and 8 are expected to increase sidewise in the corresponding [240] plane as well as in depth, depending on (a) pitting potential, (b) re-passivation potential, and (c) in-[241] hibition potential and their properties [37,38]. A corrosive environment, under fatigue loads and [242] the localised pitting in the Centaur could lead to the formation of large cavities and could become [243] one possible form of structural failure even though considerable material remains on the surfaces [244] [22,39,40]. Furthermore, in its current environment, corrosion pits in the Centaur (Figs. 6 and 8) [245] will continue their electrochemical reactions and cause inter-sub-granular corrosion, resulting in [246] stress corrosion cracking (SCC) when exposed to stresses [40,41]. Climatic effects such as oxygen, [247] water, and salts are able to promote surface corrosion [21,39] and can penetrate into the sub-[248] surface layers through the corrosion cracks (Fig. 5) delivering rapid corrosion. [249]

Significant precipitation in Bovington for 18 days of each month [42] on average has been [250] reported in terms of fog, rain, and/or snow. The relative humidity averages around 80 % for most [251]

TABLE 5—*Centaur EDS results of sub-surface crack and bulk metal.*

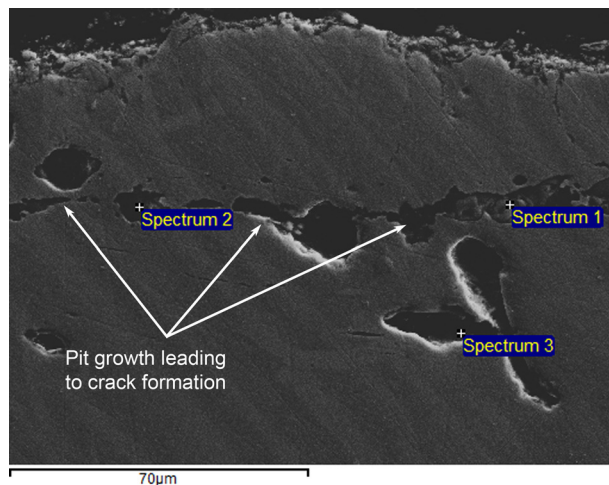|								
Sample: Centaur—Cross Sectional Surface (Results in Weight %)								
Processing Option: All Elements Analysed/Normalised								
Spectrum No.	O	Al	Si	Cr	Mn	Fe	Ni	Mo
1	0.00	0.00	0.00	1.94	0.74	96.63	0.67	0.00
2	0.00	0.00	0.42	1.90	0.47	96.42	0.76	0.00
Crack	4.36	0.86	1.58	1.87	1.23	88.21	0.65	1.20

FIG. 8—*Centaur cross section—corrosion pits in random shapes and geometries.*

of the year; however, peaks of 100 % and lows over a range of 40 %–60 % occur [43]. Average high and low temperatures for around 30 years (1981–2010) were 14.03°C and 8.11°C, respectively, whereas daily average fluctuations between 7°C to 22°C in summer and 2°C to 12°C in winter were observed [42,44].

There are 30 Acid and Aerosols Monitoring Network (AGANet) sites in the United Kingdom [45]. There is no such monitoring centre at Bovington. Therefore, the AGANet site at Goonhilly Downs was used to understand the air quality with respect to average deposition of salts and pollutants. Goonhilly Downs is situated in the Lizard Peninsula in Cornwall, England and is approximately 6 km north of the English Channel. Similar environmental conditions are expected in Bovington, which is around 9 km from the same marine environment.

The average salts and pollutants recorded between 2006 and 2009 were: chlorides at $4.0 \, \mu g/m^3$, sulphur dioxide at $0.080 \, \mu g/m^3$, sulphites at $1.00 \, \mu g/m^3$, nitrates at $3.00 \, \mu g/m^3$, sodium at $2.00 \, \mu g/m^3$, and no calcium and magnesium were found [45]. Sulphur dioxide and sulphite levels are shown to be relatively low, though they are only indirectly related to the effects of sulphur dioxide on corrosion but the actual amount of hydrated sulphur dioxide deposited on metal surfaces is important. The actual amount of sulphur deposited on the outdoor tanks will be less than the amount found in the aerosols. The atmospheric chloride concentration is low, as expected for a normal rural area.

The presence of S-containing compounds in the air and presence of S at the cross section of the Centaur will stimulate corrosion. The rust formed on the Centaur will absorb SO_2 and water from the air and the result would be the formation of sulphate-containing electrolytes. When corrosion occurs, the formation of iron sulphate ($FeSO_4$) takes place, which then reacts with oxygen resulting in iron oxy-hydroxide. Consequently, local acidity is increased by the regeneration of sulphate [13].

$$FeSO_4 + 1.5H_2O + 0.5O_2 \rightarrow FeO(OH) + 2H^+ + SO_4^{2-}$$
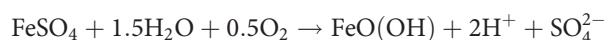
The electrochemical mechanism developed by the continuous wet–dry cycles in this natural environment, via condensation, precipitation, heat, and wind would play a significant role in the corrosion of the tanks [46,47]. Once the paint barrier is damaged and the underlying carbon steel

substrate is exposed to the environment, the activity of the corrosion reactions would be almost 278
continuous. The oxidation of the metal is known to occur in an accelerated manner during wet 279
conditions. Furthermore, the highest rate of corrosion takes place just before drying starts, i.e., 280
when the liquid layer is thin (before evaporation) and the oxygen transport through the electrolyte 281
film is maximum [13,48]. 282

The addition of chlorides and sulphurs, in the form of sulphates, sulphides, sulphites, and sul- 283
phurous salts, in the atmospheric environment, increases the corrosion rate [49–52]. Salts play 284
three main roles in accelerating corrosion: (a) they are imperfections on the surfaces and thereby 285
points of corrosion nucleation, (b) they form a hygroscopic salt film on the substrate surface that 286
keeps the surface wet for longer periods of time because the salt layer causes the surface to remain 287
wet at a lower relative humidity compared to clean surfaces, and (c) salts act to increase the con- 288
ductivity of the thin electrolyte film that drives the electrochemical reaction, i.e., corrosion [52,53]. 289

Bovington is around 9 km from the sea (English Channel), therefore, the electrolytic layer 290
formed on the surfaces of the tanks will be conductive because of the possibility of soluble chlorides 291
AQ2   and sulphates; this may result in the breakdown of protection [13,22]. Once the breakdown of the 292
protection has occurred, corrosion products, airborne salinity, and particles of hygroscopic salts 293
will influence the rate of corrosion and as a consequence deterioration of the Centaur will prevail. 294

Conclusions 295

This research work identified corrosion pits, sulphide inclusions, sub-surface corrosion cracking, 296
and progressive general corrosion on the surfaces for both the Sherman and Centaur tanks. Study 297
of the environments both inside and outside the museum has been conducted to relate corrosion 298
activity within the context. 299

Corrosion residues were relatively thick on the surfaces of the Sherman, whereas the phenom- 300
enon of sub-surface corrosion pits was widespread in the Centaur. Corrosion damage in the Cen- 301
taur is critical and can be classified as a major risk to its structural integrity. It is of great interest 302
that tanks that display surface contaminants should be conditioned. For the museum artefacts, pre- 303
ventative methods that could compromise the historic distinction of the vehicles are not viable 304
options. However, for their longevity, it is important to eliminate corrosion contaminants from the 305
surfaces, and the control of temperature and humidity is needed. 306

Close proximity of Bovington to the English Channel results in extensive rainfall, winds, tem- 307
perature fluctuations, and high humidity together with high salt content throughout the year. For 308
the outdoor tanks, it is important that any surfaces without adequate protection be protected 309
against such conditions, so their structural deterioration through corrosion can be minimised. 310

The novelty of the current research lies in the fact of fully characterising structural materials 311
where information and specifications were not complete or scarce. The current research provides 312
understanding of the failure mechanisms because of corrosion and linkages to the materials' char- 313
acteristics. These results will inform an optimised design solution of controlled environment and 314
preventative measures for the vehicles kept in uncontrolled environments. 315

Acknowledgments 316

References

[1]   Vinod, A. S., "Corrosion in the Military," *Corrosion: Environments and Industries: ASM Int.*, Vol. 13C, 2006, pp. 126–135.

[2]   Morefield, S., Drozdz, S., Hock, V., and Abbott, W., "Measuring Rates and Impact of Corrosion on DOD Equipment," *Corros. Mil. II*, Vol. 38, 2008, pp. 163–181.

[3]   Chamberlain, P. and Ellis, C., *British and American Tanks of World War II: The Complete Illustrated History of British, American, and Commonwealth Tanks, 1939–1945*, Cassell & Co., London/New York, 2000.

[4]   Jackson, R., *Tanks and Armoured Fighting Vehicles*, Parragon, Bath, 2007.

[5]   Saeed, A., Khan, Z., Garland, N., and Smith, R., "Material Characterisation to Understand Various Modes of Corrosion Failures in Large Military Vehicles of Historical Importance," *Fifth International Conference on Computational Methods and Experiments in Materials Characterisation*, Kos, Greece, June 2011, pp. 13–15.

[6]   Saeed, A., Khan, Z., Clark, M., Nel, N., and Smith, R., "Non-Destructive Material Characterisation and Material Loss Evaluation in Large Historic Military Vehicles," *Insight: Non-Destruct. Test. Cond. Monitor.*, Vol. 53, 2011, pp. 382–386.

[7]   Engel, L. and Klingele, H., *An Atlas of Metal Damage Surface Examination by Scanning Electron Microscope*, Wolfe Science/Hanser, Munich/London, 1981.

[8]   Schell, N., Martins, R. V., Beckmann, F., Ruhnau, H. U., Kiehn, R., and Schreyer, A., "The High Energy Materials Science Beamline at PETRA III," *Stress Eval. Mater. Using Neutrons Sync. Radiat.*, Vol. 571–572, 2008, pp. 261–266.

[9]   Blücher, D. B., Svensson, J. E., and Johansson, L. G., "The Influence of CO_2, $AlCl_3 \cdot 6H_2O$, $MgCl_2 \cdot 6H_2O$, Na_2SO_4 and NaCl on the Atmospheric Corrosion of Aluminum," *Corros. Sci.*, Vol. 48, 2006, pp. 1848–1866.

[10] Finlayson-Pitts, B. J. and Pitts, J. N., *Atmospheric Chemistry: Fundamentals and Experimental Techniques*, Wiley, New York, 1986.

[11] Chao, J., Capdevila-Montes, C., and González-Carrasco, J. L., "On the Delamination of FeCrAl ODS Alloys," *Mater. Sci. Eng.: A*, Vol. 515, 2009, pp. 190–198.

[12] Hylander, L. D., "Global Mercury Pollution and Its Expected Decrease after a Mercury Trade Ban," *Water, Air, Soil Pollut.*, Vol. 125, 2001, pp. 331–344.

[13] Lyon, S. B., "Corrosion of Carbon and Low Alloy Steels," *Shreir's Corrosion*, T. J. A. Richardson, Ed., Elsevier, New York, 2010, pp. 1693–1736.

[14] Williams, D. E., Kilburn, M. R., Cliff, J., and Waterhouse, G. I. N., "Composition Changes around Sulphide Inclusions in Stainless Steels, and Implications for the Initiation of Pitting Corrosion," *Corros. Sci.*, Vol. 52, 2010, pp. 3702–3716.

[15] Kiessling, R. and Lange, N., *Non-Metallic Inclusions in Steel*, 2nd ed., Metals Society, London, 1978.

[16] Pereira, A. A., Boehs, L., and Guesser, W. L., "The Influence of Sulfur on the Machinability of Gray Cast Iron FC25," *J. Mater. Proc. Technol.*, Vol. 179, 2006, pp. 165–171.

[17] Wranglen, G., "Pitting and Sulphide Inclusions in Steel," *Corros. Sci.*, Vol. 14, 1974, pp. 331–349.

[18] Bento, J. M. V., Pena, A., Lino, C. M., and Pereira, J. A., "Determination of Ochratoxin A Content in Wheat Bread Samples Collected from the Algarve and Bragança Regions, Portugal: Winter 2007," *Microchem. J.*, Vol. 91, 2009, pp. 165–169.

AQ3

[19] Jeon, S.-H., Kim, S.-T., Lee, I.-S., and Park, Y.-S., "Effects of Sulfur Addition on Pitting Corrosion and Machinability Behavior of Super Duplex Stainless Steel Containing Rare Earth Metals: Part 2," *Corros. Sci.*, Vol. 52, 2010, pp. 3537–3547.

[20] ISO 9223, "Corrosion of Metals and Alloys—Corrosivity of Atmospheres—Classification, Determination and Estimation," International Organization for Standardization, Geneva, Switzerland, 2012, p. 15.

AQ4

[21] Cai, J. P. and Lyon, S. B., "A Mechanistic Study of Initial Atmospheric Corrosion Kinetics Using Electrical Resistance Sensors," *Corros. Sci.*, Vol. 47, 2005, pp. 2956–2973.

[22] Schweitzer, P. A., *Fundamentals of Corrosion: Mechanisms, Causes, and Preventative Methods*, CRC, Boca Raton, FL, 2010.

[23] Trethewey, K. R. and Chamberlain, J., *Corrosion: For Students of Science and Engineering*, Longman Scientific & Technical, Harlow, U.K., 1988.

[24] Kart, H. H., Uludogan, M., and Cagin, T., "DFT Studies of Sulfur Induced Stress Corrosion Cracking in Nickel," *Comput. Mater. Sci.*, Vol. 44, 2008, pp. 1236–1242.

[25] Williams, D. E., Mohiuddin, T. F., and Zhu, Y. Y., "Elucidation of a Trigger Mechanism for Pitting Corrosion of Stainless Steels Using Submicron Resolution Scanning Electrochemical and Photoelectrochemical Microscopy," *J. Electrochem. Soc.*, Vol. 145, 1998, pp. 2664–2672.

[26] Eklund, G. S., "Initiation of Pitting at Sulphide Inclusions in Stainless Steel," *J. Electrochem. Soc.*, Vol. 121, 1974, pp. 467–473.

[27] Greenwood, N. N. and Earnshaw, A., *Chemistry of the Elements*, 2nd ed., Butterworth-Heinemann, Oxford, 1997.

[28] Castaño, J. G., Botero, C. A., Restrepo, A. H., Agudelo, E. A., Correa, E., and Echeverría, F., "Atmospheric Corrosion of Carbon Steel in Colombia," *Corros. Sci.*, Vol. 52, 2010, pp. 216–223.

[29] Kamimura, T., Hara, S., Miyuki, H., Yamashita, M., and Uchida, H., "Composition and Protective Ability of Rust Layer Formed on Weathering Steel Exposed to Various Environments," *Corros. Sci.*, Vol. 48, 2006, pp. 2799–2812.

[30] Dillmann, P., Mazaudier, F., and Hœrlé, S., "Advances in Understanding Atmospheric Corrosion of Iron: I. Rust Characterisation of Ancient Ferrous Artefacts Exposed to Indoor Atmospheric Corrosion," *Corros. Sci.*, Vol. 46, 2004, pp. 1401–1429.

[31] Ma, Y., Li, Y., and Wang, F., "The Effect of β-FeOOH on the Corrosion Behavior of Low Carbon Steel Exposed in Tropic Marine Environment," *Mater. Chem. Phys.*, Vol. 112, 2008, pp. 844–852.

[32] Williams, D. E., Westcott, C., and Fleischmann, M., *Stochastic Models of Pitting Corrosion of Stainless Steels: Part 1; Modelling of the Initiation and Growth of Pits at Constant Potential*, UKAEA Atomic Energy Establishment Materials Development Division, Harwell, 1984.

[33] Williams, D. E., Westcott, C., and Fleischmann, M., *Stochastic Models of Pitting Corrosion of Stainless Steels: Part 2; Measurement and Interpretation of Data at Constant Potential*, UKAEA Atomic Energy Establishment Materials Development Division, Harwell, 1984.

[34] Williams, D. E., Westcott, C., and Fleischmann, M., "Studies of the Initiation of Pitting Corrosion on Stainless Steels," *J. Electroanal. Chem. Interfacial Electrochem.*, Vol. 180, 1984, pp. 549–564.

[35] Williams, J. A., "Wear and Wear Particles—Some Fundamentals," *Tribol. Int.*, Vol. 38, 2005, pp. 863–870.

[36] Alvarez, M. G. and Galvele, J. R., "Pitting Corrosion," *Shreir's Corrosion*, T. J. A. Richardson, Ed., Elsevier, New York, 2010, pp. 772–800.

[37] Baboian, R., *Automotive Corrosion Tests and Standards*, Society of Manufacturing Engineers, Dearborn, MI, 1996.

[38] Askey, A., Lyon, S. B., Thompson, G. E., Johnson, J. B., Wood, G. C., Sage, P. W., et al, "The Effect of Fly-Ash Particulates on the Atmospheric Corrosion of Zinc and Mild Steel," *Corros. Sci.*, Vol. 34, 1993, pp. 1055–1081.

[39] Turnbull, A., McCartney, L. N., and Zhou, S., "A Model to Predict the Evolution of Pitting Corrosion and the Pit-to-Crack Transition Incorporating Statistically Distributed Input Parameters," *Corros. Sci.*, Vol. 48, 2006, pp. 2084–2105.

[40] Horner, D. A., Connolly, B. J., Zhou, S., Crocker, L., and Turnbull, A., "Novel Images of the Evolution of Stress Corrosion Cracks from Corrosion Pits," *Corros. Sci.*, Vol. 53, 2011, pp. 3466–3485.

[41] Weather Underground, 2011, http://www.wunderground.com/weatherstation/WXDailyHistory.asp?ID=IDORSETB5 (Last accessed 21 Nov 2011).

[42] Metoffice, 2011, "Station Data," http://www.metoffice.gov.uk/climate/uk/stationdata/hurndata.txt (Last accessed 21 Nov 2011).

[43] dorsetforyou.com, 2012, "Climate Data for Weymouth, England (1981–2010)," http://webapps-wpbc.dorsetforyou.com/apps/weather/annualreport.asp.

[44] Defra, 2011, "Acid Gas and Aerosol Network (AGANet)," http://uk-air.defra.gov.uk/networks/network-info?view=aganet (Last accessed 24 Nov 2011).

[45] Stratmann, M., Bohnenkamp, K., and Engell, H. J., "An Electrochemical Study of Phase-Transitions in Rust Layers," *Corros. Sci.*, Vol. 23, 1983, pp. 969–985.

[46] Stratmann, M., Bohnenkamp, K., and Ramchandran, T., "The Influence of Copper upon the Atmospheric Corrosion of Iron," *Corros. Sci.*, Vol. 27, 1987, pp. 905–926.

[47] Alwash, S. H., Ashworth, V., Shirkhanzadeh, M., and Thompson, G. E., "An Investigation of the Reduction of Oxygen at a Rotating Disc Electrode With Heat Transfer Facilities," *Corros. Sci.*, Vol. 27, 1987, pp. 1301–1311.

[48] El-Mahdy, G. A., Nishikata, A., and Tsuru, T., "Electrochemical Corrosion Monitoring of Galvanized Steel under Cyclic Wet–Dry Conditions," *Corros. Sci.*, Vol. 42, 2000, pp. 183–194.

[49] Nishikata, A., Yamashita, Y., Katayama, H., Tsuru, T., Usami, a., Tanabe, K., et al, "An Electrochemical Impedance Study on Atmospheric Corrosion of Steels in a Cyclic Wet–Dry Condition," *Corros. Sci.*, Vol. 37, 1995, pp. 2059–2069.

[50] Yadav, A. P., Nishikata, A., and Tsuru, T., "Electrochemical Impedance Study on Galvanized Steel Corrosion under Cyclic Wet–Dry Conditions—Influence of Time of Wetness," *Corros. Sci.*, Vol. 46, 2004, pp. 169–181.

[51] Schwitter, H. and Bohni, H., "Influence of Accelerated Weathering on the Corrosion of Low-Alloy Steels," *J. Electrochem. Soc.*, Vol. 127, 1980, pp. 15–20.

[52] Corvo, F., Mendoza, A. R., Autie, M., and Betancourt, N., "Role of Water Adsorption and Salt Content in Atmospheric Corrosion Products of Steel," *Corros. Sci.*, Vol. 39, 1997, pp. 815–820.

[53] Neufeld, A. K., Cole, I. S., Bond, A. M., and Furman, S. A., "The Initiation Mechanism of Corrosion of Zinc by Sodium Chloride Particle Deposition," *Corros. Sci.*, Vol. 44, 2002, pp. 555–572.